Display and Imaging, Vol. 2, pp. 93–106
Reprints available directly from the publisher
Photocopying permitted by license only

Optical properties of self-assembled aluminum phthalocyanine chloride thin films

A. ZAWADZKA[1*], P. PŁÓCIENNIK[1], D. GUICHAOUA[2], S TABOUKHAT[2,3], A. KORCALA[1] AND B. SAHRAOUI[2]

[1]*Institute of Physics, Faculty of Physics, Astronomy and Informatics, Nicolaus Copernicus University, Grudziadzka 5, 87-100 Torun, Poland*
[2]*LUNAM Université, Université d'Angers, CNRS UMR 6200, Laboratoire MOLTECH-Anjou, 2 bd Lavoisier, 49045 ANGERS cedex, France*
[3]*Laboratory of Materials Engineering and Biosciences, ENS, University Hassan II, Casablanca, Morocco*

Received: October 8, 2015. Accepted: November 8, 2015

Optical and structural investigations of the aluminum phthalocyanine chlorides thin films are presented. The films were fabricated by vacuum sublimation technique onto quartz substrates and annealed after fabrication in an ambient atmosphere for 24 hours at the temperature equal to 250°C. The linear optical properties of the thin films were studied by the measurements of the transmission and reflection spectra at the normal incidence of the light in the spectral range 200-2000nm. We show that the linear optical properties are dependent on the thin film's structure. Experimental results were used for theoretical calculations of the dispersion and absorption parameters for the films. We found that the annealing process changes the value of the optical band gaps and causes formation of nanostructures what makes this material interesting for future optical applications.

Keywords: Aluminum Phthalocyanine Chloride, Optical Properties, Annealing Process, Nanostructural Thin Films

1. INTRODUCTION

Over the last years, phthalocyanines and metallophthalocyanine complexes have been intensively investigated due to their unusual physical and thermal

*Corresponding author: azawa@ fizyka.umk.pl

properties [1-3]. Phthalocyanine is an organic compound that forms stable complexes with several metals that have long been known as blue or green dyes and pigments. The metallophthalocyanine chlorides are not only pigments, but also nontoxic p-type organic semiconductors with good thermal and chemical stability. These materials are extremely attractive for use in optical and electronic devices. The performances of these devices are strongly dependent on the nature of the material and its processing, design as well as deposition technique.

For most metallophthalocyanine chlorides, five transition bands, labeled as Q and B (Soret), N, L and C bands were identified [4-7]. Some complexes may miss one or two of these bands. The absorption spectra of metallophthalocyanine chlorides have been studied in vapor form [8-9], solution [10-11] and solid state [12–13]. However, understanding and explaining of the complexes' optical properties are still far from complete. Optical properties of unsubstituted phthalocyanine as well as complexes depend on molecular properties such as an atomic number, position and nature of substitute atoms. Type of the central metal and its position relative to the ligand's ring play very important role and significantly affect the physical properties. Metal-free phthalocyanine forms completely planar molecule structure. Most of the phthalocyanine complexes have a planar coordination around the central ion, which means that the metal and ligand atoms are generally in one plane. These molecules possess approximately D_{4h} symmetry [14]. The structure of the metallophthalocyanine chlorides differs from metal-free phthalocyanine and is much similar to the metallophthalocyanine oxides. The metal's atom lies out of the Pc macrocycle plane and the Cl atom is in extra-coordination position, giving these molecules approximately C_{4v} symmetry [15]. Additionally, the plane of the molecule is slightly domed.

The molecular structure of the aluminum phthalocyanine chloride, presented on Fig.1, is just the unique central symmetric planar structure of the 16 members ring with 18 delocalized π-electrons which leads to their exceptional optical properties and extraordinary stability. Most of the metallophthalocyanines and its complexes can form different nanostructures and different crystalline structure. The main difference between them is arrangement of the common columns in the crystalline structure and the tilt angle of the molecule within the columns. Thus, the obtained thin films possessing different tilt angle of the molecule lead to different structural and optical properties [16–17].

This paper is devoted to optical and structural properties of the aluminum phthalocyanine chlorides thin films fabricated by vacuum sublimation technique on quartz substrate and their dependences on the temperature applying during the annealing process. Factors such as fabrication's technique or morphology of the film and the temperature of the annealing process are very important for the performance of potential optical or electronic devices.

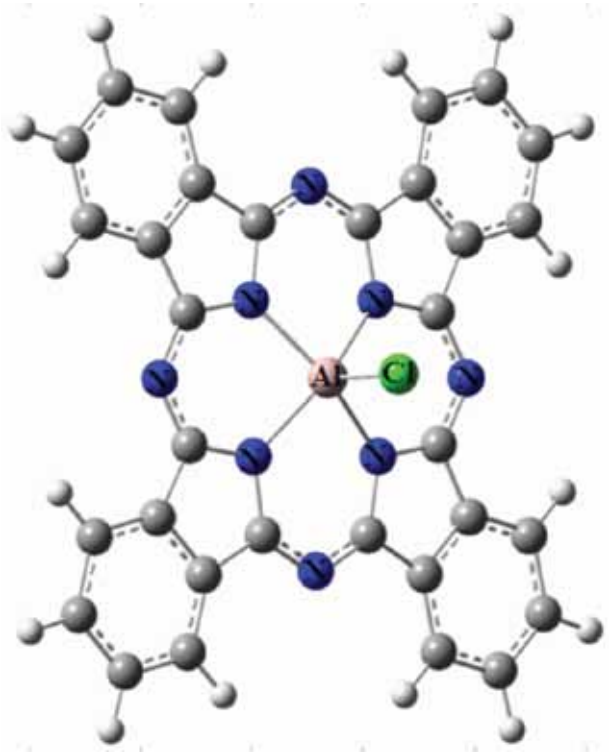

FIGURE 1
Molecular structure of the aluminum phthalocyanine chloride.

2. EXPERIMENT

Aluminum phtalocyanine chloride (AlClPc) thin films were fabricated by vacuum sublimation technique [18–19]. Thin films were deposited on the quartz substrates. The deposition process was prepared in vacuum chamber under pressure about $5*10^{-5}$ Pa. The source material was thermally evaporated from quartz effusion cell with a nozzle of 10 mm in diameter on the top and heated by tungsten resistance coil. The main factors influencing the film's thickness during thermal evaporation process were time of evaporation and distance between source and substrate. In the case of this experimental system the manual-control deposition assures approximately 95% accuracy of desired film thickness value. Source material used for this high vacuum's deposition was supplied by Sigma Aldrich Co. and used as received. The distance between the source and the substrate was about 10cm and substrate was held at room temperature during evaporation. Selected thin films were annealed after the deposition process to obtain the different structural properties. The annealing process was carried out in ambient atmosphere at temperature of 250^{o}C and lasted 24 hours.

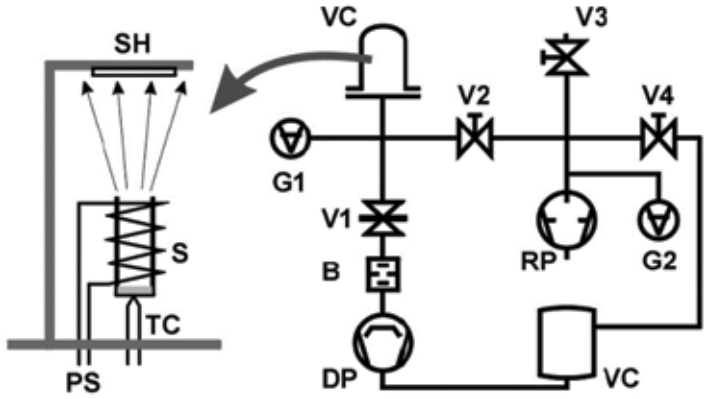

FIGURE 2
Vacuum sublimation set-up. Left part - evaporation equipment: S – source (effusion cell and heater), SH – sample (substrate) holder, TC – K-type thermocouple, PS – power supply. Right part – scheme of vacuum system: VC – vacuum chamber, V1-4 – manual valves, B – baffle, G1-2 – vacuum gauges, VC – equalization vacuum chamber, RP – sliding vane rotary vacuum pump, DP – diffusion pump.

3. RESULTS AND DISCUSSION

Figure 3 presents the measurements of XRD (2θ scan) of the studied AlClPc thin films deposited on the substrate kept at room temperature during the depositions process and next annealed at the temperature equal to 250°C. The 2θ scan process is sensitive to both reflections from parallel planes to the sample surface and others not fulfilling this condition. In the case of this experiment, all measurements were carried out by diffractometer using CuK_α ($\lambda = 0.1542$nm) radiation [20-21].

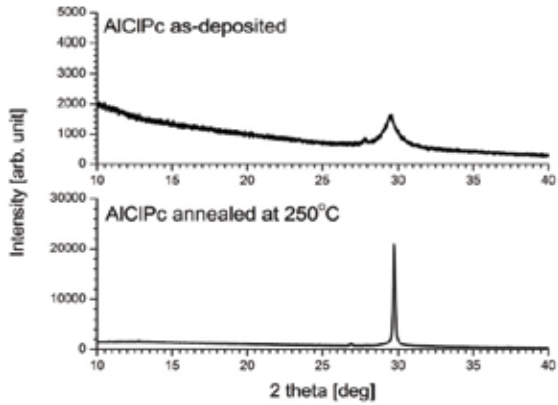

FIGURE 3
XRD spectra of AlClPc thin film: as-deposited sample and annealed at temperature of 250°C.

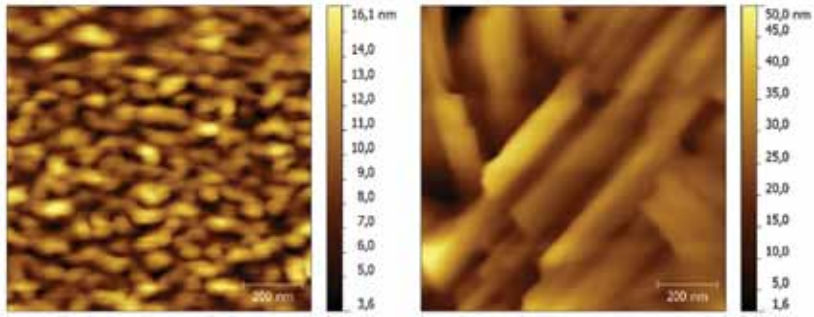

FIGURE 4
The topographic AFM images (1μm x 1μm) of a AlClPcs nanostructures for: (a) as-deposited samples AlClPc and the same samples after annealing process at temperature equal to 250°C (b).

For the as-deposited AlClPc thin film there are two small and relatively wide peaks: one with the maximum at $2\theta = 29.520°$ and second at 27.724°. For the sample annealed at a temperature equal to 250°C two peaks are also observed, but the location and intensity of each one behaves differently as the temperature increases. The position of the first peak is slightly shifted toward larger values of the 2θ angle, the maximum of the peak is located at $2\theta = 29.723°$ and the intensity of the peak is about 15 higher. The position of the second peak is much more shifted toward smaller values of the 2θ angle, the maximum of the peak is located at $2\theta = 26.886°$ and the intensity of the peak is comparable. For all annealed films, the intensity of the peaks increased with increasing annealing temperature and location of the peaks shifted mostly towards larger values of the 2θ angle. The growth of the peaks intensity leads to the conclusion, that higher annealing temperature causes the higher level of the crystal structure arrangement. This phenomenon can be explained by an increase in mobility of the particles with increasing temperature. The particles have higher surface mobility in higher temperature, which provides the possibility of taking up defined positions on the surface.

During the deposition process evaporated particles are usually randomly dispersed inside the plume and form randomly ordered nanostructures on the substrate's surface. AlClPcs molecules are adsorbed on the substrate after several seconds since the immersion of the substrate plate. A typical image of the thin film surface after the deposition is shown in Fig. 4a. Application of the annealing process immediately after the deposition allows specifying geometry of the particles assembly and therefore self-assembled organometallic nanostructure's formation [22]. Self-assembly is an equilibrium process, where the assembled particles are in equilibrium with the surrounding components and driven by the minimization of the Gibbs free energy. The minimization of this energy is attained by the minimization of repulsive and the maximization of attractive molecular interactions. In addition, the lower

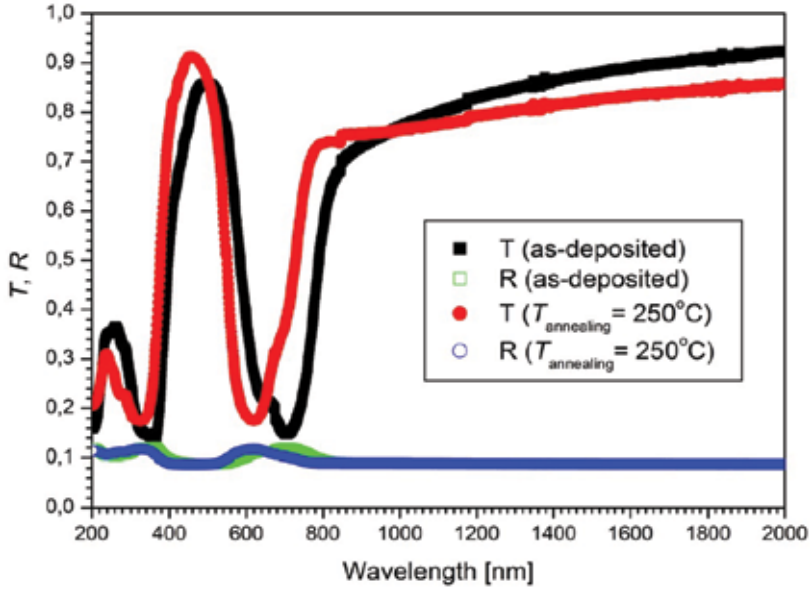

FIGURE 5
Transmission T and reflection R spectra of AlClPc thin film fabricated by a vacuum sublimation process on the quartz substrate as a function of the incident wavelength and temperature of the annealing process.

free energy is usually a result of a weaker intermolecular force between self-assembled moieties in the nature. In the case of this experiment, the process of self-assembled nanostructures formation took 24 hours and was carried out in ambient atmosphere at the temperature equal to 250°C. This temperature and this time's period allowed achieving the ideal arrangement of molecules consisting of finding the minimum free energy of the system and optimizing all the complicated interactions between the adsorbed AlClPcs molecules. Using the annealing process, we obtained nanostructures with a specific arrangement almost parallel to the substrate, as illustrated in Fig. 4b. These nanorods structures are especially interesting for optical applications and optical or thermal sensing. This irreversible thermal-induced self-assembly process is versatile, as a single assembly system can pattern multiple geometries by simply controlling the external thermal conditions [2, 23]. Spatial arrangements of these self-assembled nanostructures can be potentially used to build increasingly complex structures leading to a wide variety of materials that can be used for different purposes.

Mutual arrangement of the molecules plays paramount role for optical properties of the material. The knowledge of the linear optical properties such as: refractive index and proportional to the complex refractive index absorption coefficient is essential for applications in modern optical technologies. Figure 5 shows the spectral distributions of the transmittance

(T) and the reflectance (R) measured at normal incidence in the spectral range 200–2000 nm using a home-made one-beam spectrometer [24-26]. The thickness of all investigated samples was equal to 100nm. All experimental spectra can be simply divided into two regions: 200–850nm and 850–2000nm. Inside the first region, total sum of the transmittance and the reflectance is greater than 0.9 suggesting very good optical transparency of the films. Inside the second region the total sum is much less than 1 what implies that the films can be considered as good light absorbers.

Review of the Fig.5 shows that the transmittance (T) as well as the reflectance (R) of films changing intensity after annealing process with changing position of all peaks. Transmittance for AlClPcs compounds after annealing at 250°C decreases in comparison with transmittance of samples without applying this process. Annealing process shifts also the peak position of all bands towards high wavelength side of the spectra. For all experimental spectra, four absorption bands take notations Q, B, N and C were observed. The Q-band exists in the visible region of spectra and corresponds to the transition between the ground state $I_{au}(\pi)$ HOMO and the state e_g (π^*) LUMO while others (B, N and C) exist in the UV region of spectra. It is also noted that the bands B, N and C appear with intensities that are comparatively higher than of Q-band.

The absolute value of the transmission T can be described by the relation:

$$T = \left(\frac{I_{fs}}{I_s}\right)\left(1 - R_s\right) \tag{1}$$

where: I_{fs} and I_s are intensities of the radiation passes through the set fil + substrate and the clean substrate (quartz), respectively, and R_s is the reflectance of the substrate. The other hand the absolute value of reflectance R is expressed as:

$$R = \left(\frac{I_{fr}}{I_m}\right)R_m\left[1 + \left(1 - R_s\right)^2\right] - T^2R_s, \tag{2}$$

where: I_{fr} is the intensity of the radiation reflected from the sample, I_m is the intensity of the radiation reflected from the reference mirror and R_m is its reflectivity [27].

The absorption coefficientα, the extinction coefficient κ and the refractive index n of the thin film may then be calculated from equations (3) – (5) as:

$$\alpha = \frac{1}{d} ln\left[\frac{\left(1 - R\right)^2}{2T} + \sqrt{R^2 + \frac{\left(1 - R\right)^4}{4T^2}}\right] \tag{3}$$

$$\kappa = \frac{\alpha\lambda}{4\pi}, \tag{4}$$

$$n = \left[\frac{1+R}{1-R} + \sqrt{\frac{4R}{(1-R)^2} - \kappa^2}\right], \tag{5}$$

where d is the films thickness [28-30]. Figures 6, 7 and 8 show the dependences of the refractive index n, the extinction coefficient κ and the absorption coefficient α as a function of the incident radiations wavelength λ and temperature of the annealing process, respectively.

Refractive index spectra show two peaks in the ultraviolet and visible regions (about 320 and 605nm for as-deposited sample and 350 and 700nm for annealed sample). It means that the refractive index exhibits anomalous dispersion behavior for the wavelength less than 850 nm, what can be explained using the multi-oscillator model [31]. For the wavelength higher than 850 nm the refractive index decreases slowly with increasing the wavelength. Thus the refractive index exhibits normal dispersion behavior, what can be explained by the single oscillator model [32].

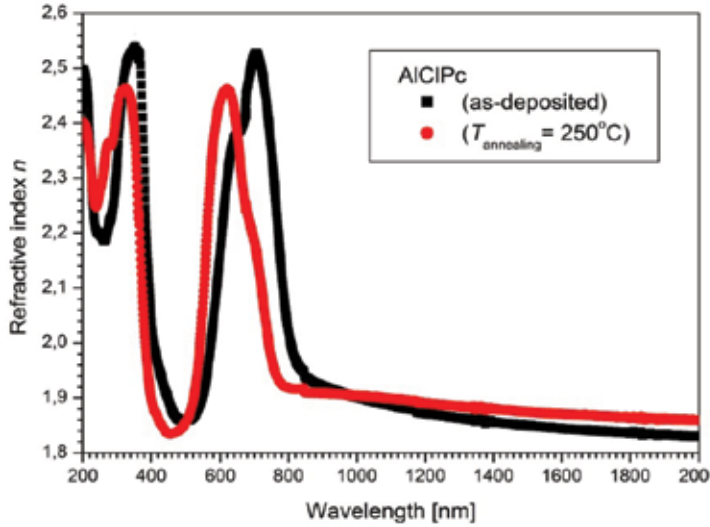

FIGURE 6
Refractive index n as a function of the incident wavelength λ for AlClPc thin film before and after annealing process.

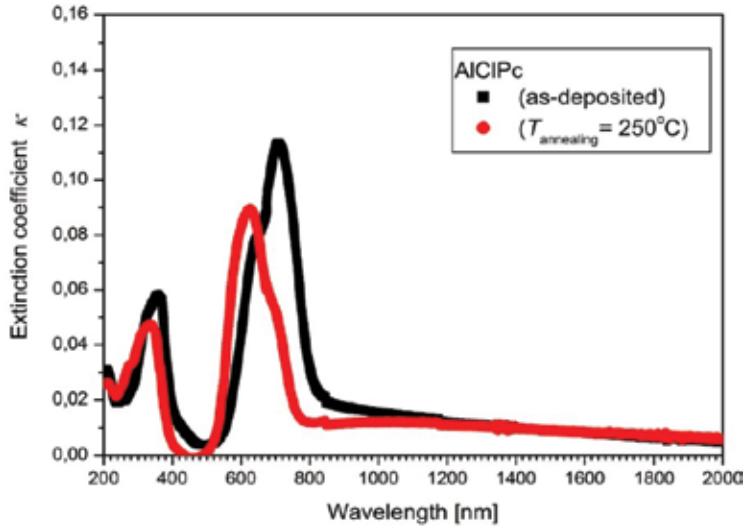

FIGURE 7
Extinction coefficient κ as a function of the incident wavelength λ for AlClPc thin film.

The dependence chart of the absorption coefficient α for the as-deposited sample and then subjected to the annealing process has three main peaks. The maxima of the peaks are equal to energies: 1.72, 3.51 and 5.58eV. After the

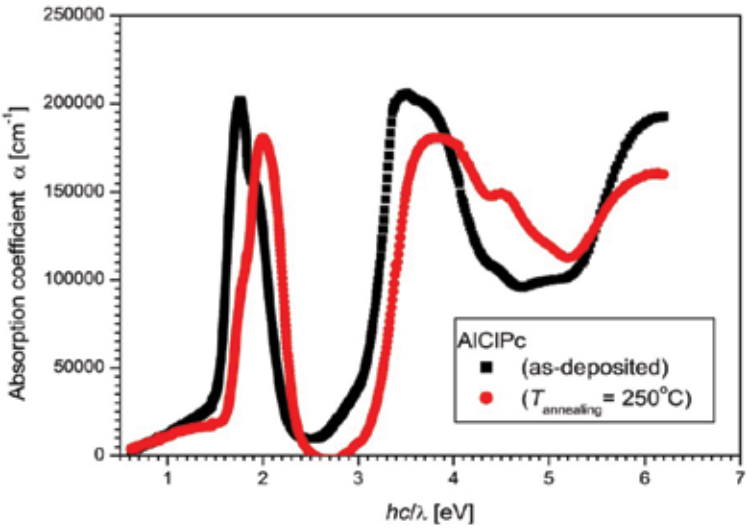

FIGURE 8
Absorption coefficient α as a function of the incident radiations energy for AlClPc thin film.

annealing process, the whole spectrum shifts towards higher energies and absorption maxima are for the 2.0, 3.8 and 6eV. The first of these values is associated with the Q-band, the second and the third with the Soret and N bands, respectively. As can be seen from the obtained graph, the absorption coefficient for each of these bands is comparable and annealing process can specifically split Soret band.

Analysis of the absorption coefficient α as a function of the photon energy near the absorption edge allows determining the optical band gap and type of the optical transition for both crystalline and non-crystalline materials. This can be achieved by using the relation (6) also known as Tauc plot [33]:

$$\alpha h\frac{c}{\lambda} = a'\left(\frac{hc}{\lambda} - E_g\right)^f, \tag{6}$$

where h is Planck's constant, c – the speed of light, E_g – the value of the optical energy gap. The value of the exponent f denotes the nature of the transition [34]: $f = 1/2$ for direct allowed transitions, $f = 3/2$ for direct forbidden transitions, $f = 2$ for indirect allowed transitions and $f = 3$ for indirect forbidden transitions. Constant a' is a parameter that depends on the optical transition probabilities.

Figure 9a-b presents an analysis of Tauc plots for as-deposited (a) and annealed at 250°C (b) AlClPc thin film inside the range of the strong absorption. The best fitting of the experimental data to equation (6) was obtained for the direct allowed transition regardless whether the thin film has been subjected to the annealing process or not. The optical band gap and the trap's levels were determined as 1.58, 3.11 and 5.12eV for as-deposited sample and 1.72, 3.28 and 4.85 for thin film annealed at 250°C. Two first peaks shifted to larger energies and third to lower energy. This indicates that the thin films exhibited polycrystalline character and the annealing process irreversibly leads to a polycrystalline phase change [5].

Obtained spectra of the refractive indices and extinction coefficients allow calculating the real and imaginary parts of the complex dielectric constant by using following relations [35]:

$$Re(\varepsilon) = n^2 - \kappa^2, \tag{7a}$$

$$Im(\varepsilon) = 2n\kappa, \tag{7a}$$

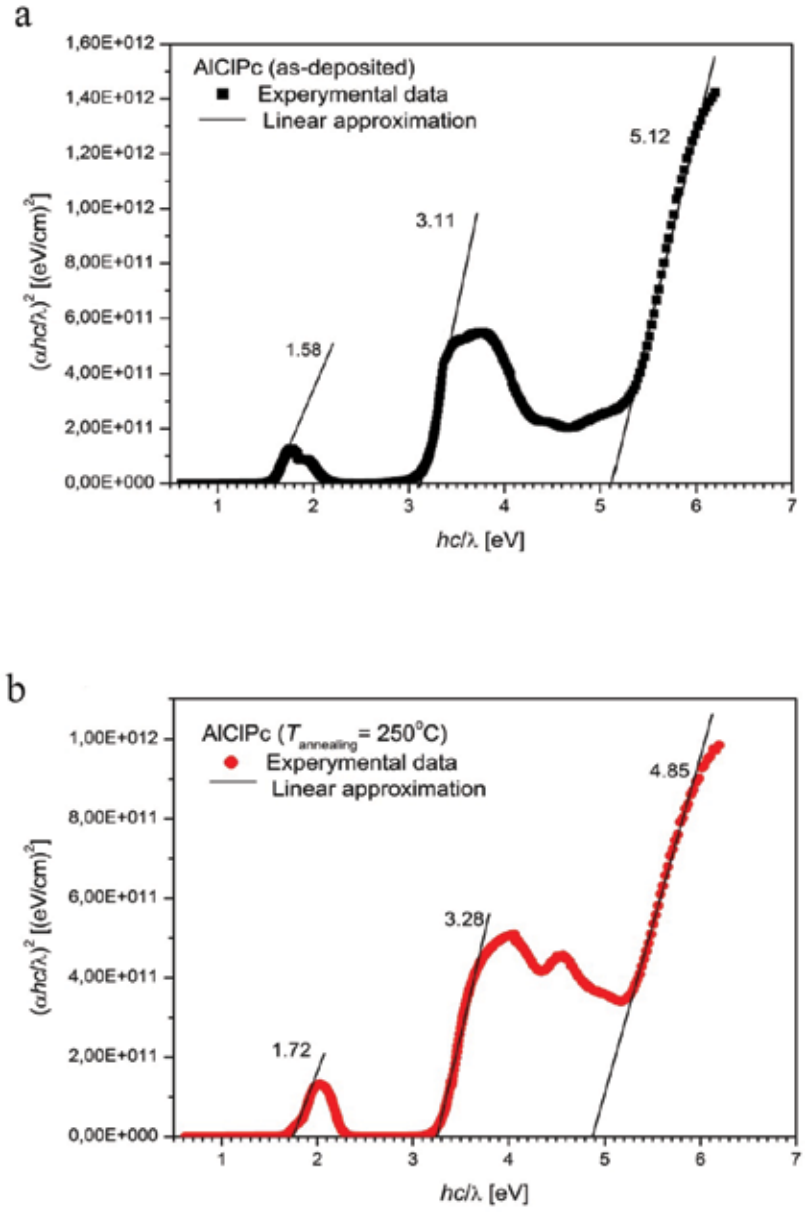

FIGURE 9
Tauc plot of as-deposited (a) and annealed at 250°C AlClPc thin film (b).

The spectra of photon energy dependencies of real and imaginary parts of the complex dielectric constant for AlPcCl thin films are shown in Fig. 10a-b. Analysis of the spectra shows that real and imaginary parts follow the same

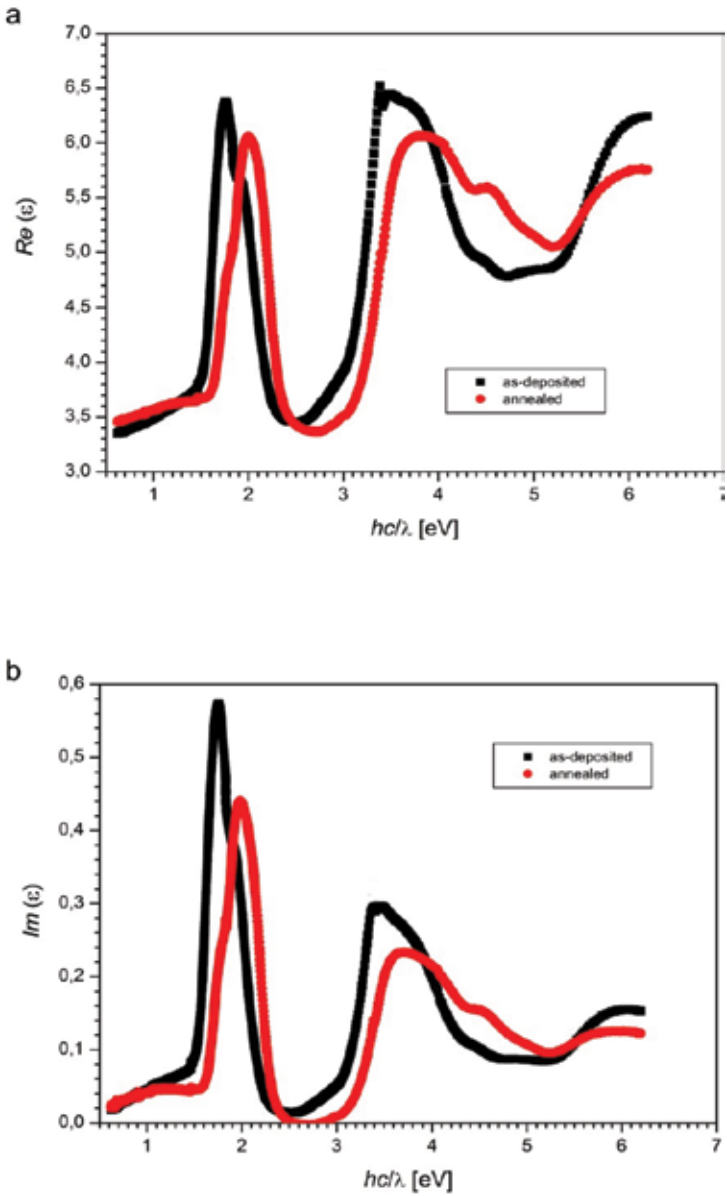

FIGURE 10
Real and imaginary parts of the dielectric constant for AlPcCl thin film as a function of photon energy.

pattern and the values of the real part are about ten times higher than the imaginary part. Moreover, the variation of the dielectric constant as a function of the photon energy indicates that some inter-actions between photons and electrons inside thin films.

4. CONCLUSION

Presented transmittance and reflectance spectra showed that the AlPcCl nanostructured thin films absorb the light waves in the wavelength range 200–850 and are optically transparent within the spectral range 850–2000nm. Optical absorption spectra shows three absorption peaks located at about 2, 3.5 and 6.5eV. Tauc plots for the films exhibit direct allowed band-band and inter-band transitions. Estimated optical band gaps are equal to 1.58, 3.11 and 5.12eV for as-deposited sample and 1.72, 3.28 and 4.85eV for thin film annealed at 250^{o}C, which is in the range of other metallophthalocyanine thin films. Refractive index exhibits anomalous dispersion in the spectral range 200–850nm and normal dispersion in the spectral range 850–2000nm. Obtained results allowed calculating real and imaginary parts of the dielectric constant their dependence on the photon energy, indicating some interactions between the photons and the electrons inside thin films.

REFERENCES

[1] F. Hacivelioglu, M Durmus, S Yesilot, A. Gül Gürek, A. Kilic and V. Ahsen, *Dyes Pigm.* **79**, 14-23, 2008.

[2] A. Zawadzka, P. Płóciennik, J. Strzelecki, A. Korcala, A.K. Arof, B. Sahraoui, *Dyes Pigm.* **101**, 212-220, 2014.

[3] M.M. El-Nahass, H.M. Zeyada, M.S. Aziz and N.A. El-Ghamaz, *Opt. Mater.* **27**, 491-498, 2004

[4] P. A. Chollet, F. Kajzar, J. Le Moigne, *Molecular Engineering* **1**, 35-47, 1991.

[5] M-S Liao and S Scheiner, *J. Chem. Phys.*, **114**, 9780-9791, 2001.

[6] A. Zawadzka, P. Płóciennik, I. Czarnecka, J. Sztupecka, Z. Łukasiak, *Opt. Mater.* **34**, 1686-1691, 2012.

[7] A. Zawadzka, A. Karakas, P. Płóciennik, J. Szatkowski, Z. Łukasiak, A. Kapceoglu, Y. Ceylan, B. Sahraoui, *Dyes Pigm.* **112**, 116-126, 2015.

[8] F. I. Bohrer, C. N. Colesniuc, J. Park, M. E. Ruidiaz, I. K. Schuller, A. C. Kummel and W. C. Trogler, *J. AM. CHEM. SOC.* **131**, 478-485, 2009.

[9] P. P. Semyannikov, T. V. Basova, V. M. Grankin and I. K. Igumenov, *Journal of Porphyrins and Phthalocyanines*, **4**, 271-277, 2000.

[10] N. B Chaure, A. N Cammidge, I. Chambrier, M. J. Cook, M. G. Cain, C. E. Murphy, C. Pal and A. K. Ray, *Sci. Technol. Adv. Mater.* **12**, 025001, 2011.

[11] S. Hu, R. Tian, Y. Dong, J. Yang, J. Liu and S. Cao, *RSC Adv*. **3**, 21447-21452, 2013.

[12] A. Zawadzka, P. Płóciennik, J. Strzelecki, Z. Łukasiak, A. Korcala, B. Sahraoui, "Optical properties of metallophthalocyanine compounds thin films", Published in: Transparent Optical Networks (ICTON), 2012 14th International Conference on, ISSN: 2161-2056, E-ISBN: 978-1-4673-2227-0, Print ISBN: 978-1-4673-2228-7, INSPEC Accession Number: 12908171, IEEE 1-3, DOI: 10.1109/ICTON.2012.6253720

[13] M. Iwase, A. Suzuki, T. Akiyama, T. Oku, *Materials Sciences and Applications*, **5**, 278-284, 2014.

[14] S. Kahlal, A. Mentec, A. Pondaven, M. L'Her and J-Y. Saillard, *New J. Chem* **33**, 574-582, 2009.

[15] D. R. Tackley, G. Dent, W. Ewen Smith Phys. Chem. Chem. Phys. **3** 1419 (2001)

[16] A. Zawadzka, P. Płóciennik, J. Strzelecki, M. Pranaitis, S. Dabos-Seignon, B. Sahraoui, *Thin Solid Films* **545**, 429-437, 2013).

[17] R S Dygdala, K Karasek, K Stefanski, A Zawadzka, R Rumianowski and M Zielinski, . *Phys. D: Appl. Phys.* **33**, 41-53, 2000.
[18] A. Zawadzka, P. Płóciennik, J. Strzelecki, Z. Łukasiak, B. Sahraoui, *Opt. Mater.* **36**, 91-97, 2013.
[19] A. Zawadzka, P. Płóciennik, J. Strzelecki, *Opt. Quantum Electron.* **46**(1), 87-101, 2014.
[20] A. Zawadzka, P. Płóciennik, J. Strzelecki, B. Sahraoui, *Opt. Mater.* **37**, 327-337, 2014.
[21] M.M. El-Nahass, H.S. Soliman, B.A. Khalifa, I.M. Soliman, *Materials Science in Semiconductor Processing*, **38**, 177-183, 2015.
[22] S. K. Hämäläinen , M. Stepanova , R. Drost , P. Liljeroth , J. Lahtinen and J. Sainio, *Phys. Chem. C*, **116** (38), 20433-20437, 2012,
[23] C. M. Drain, A. Varotto and I. Radivojevic, *Chem Rev.* **109**, 1630-1658, 2009.
[24] A. Zawadzka, P. Płóciennik, Y. El Kouari, H. Bougharraf, B. Sahraoui, *J. Lumin.*, Available online 29 April 2015, ISSN 0022-2313, http://dx.doi.org/10.1016/j.jlumin.2015.04.020.
[25] V. Serbezov, S. Sotirov, K. Benkhouja, A. Zawadzka, B. Sahraoui, *Opt. Mater.* **36**, 53-59, 2013.
[26] R.S. Dygdała ., M. Zieliński, P. Płóciennik, A. Zawadzka, R. Rumianowski , *Surf. Coat. Technol.* **203**; 2328-2332, 2009.
[27] M.M.El- Nahass, M.M.Abd El-Raheem, A.A. Atta, A.M. Hassanien, *Radiat. Phys. Chem.* **103**, 227-233, 2014
[28] M. Di Giulio, G. Micocci, R. Rella, , P. Siciliano, A. Tepore, *Phys. Status Solidi A* **136**, K101, 1993.
[29] K. Takanabe in *Solar Energy for Fuels* (*Tom 371 Topics in Current Chemistry,* ed. H. Tüysüz, C. K. Chan) Springer 2015.
[30] M.M. El-Nahass, A.A. M. Farag, M. El-Metwally, F.S.H. Abu-Samaha, E. Elesh, *Synth. Met.* **195**, 110-116, 2014.
[31] S.H. Wemple, M. Di Domenico, *Phys. Rev. B* **3**, 1338-1351, 1970.
[32] A. Stendal, U. Beckars, S. Wilbrand, O. Stenzel, C. Von Borczyskowski, *J. Phys. B: At. Mol. Opt. Phys.* **29**, 2589-2595, 1996.
[33] J. Tauc, *Materials Research Bulletin* **3**, 37-46, 1968.
[34] Davis, E. A.; Mott, N. F.. *Philosophical Magazine A* **22**(179), 903-922, 1970.
[35] R. Al Asmar, G. Ferblantier, F. Mailly, P. Gall-Borrut, A. Foucaran, *Thin Solid Films* **473** 49-53, 2005.